

## Elastic properties of grafted microtubules

Francesco Pampaloni<sup>1,5</sup>, Gianluca Lattanzi<sup>2,3,4</sup>, Alexandr Jonás<sup>5</sup>,

Thomas Surrey<sup>1</sup>, Erwin Frey<sup>6</sup> and Ernst-Ludwig Florin<sup>5\*</sup>

<sup>1</sup>*EMBL, Cell Biology and Biophysics Programme,*

*Meyerhofstr. 1, D-69117 Heidelberg, Germany*

<sup>2</sup>*Department of Medical Biochemistry, Biology and Physics, Bari, Italy*

<sup>3</sup>*TIRES-Center of Innovative Technologies for Signal*

*Detection and Processing, Università di Bari, Bari, Italy*

<sup>4</sup>*Istituto Nazionale di Fisica Nucleare, Sezione di Bari, Bari, Italy*

<sup>5</sup>*Center for Nonlinear Dynamics, University of Texas at Austin, Austin, Texas 78712 (USA)*

<sup>6</sup>*Arnold Sommerfeld Center and CeNS, Department of Physics,*

*Ludwig-Maximilians-Universität München,*

*Theresienstrasse 37, D-80333 München, Germany*

(Dated: February 9, 2008)

### Abstract

We use single-particle tracking to study the elastic properties of single microtubules grafted to a substrate. Thermal fluctuations of the free microtubule's end are recorded, in order to measure position distribution functions from which we calculate the persistence length of microtubules with contour lengths between 2.6 and 48  $\mu\text{m}$ . We find the persistence length to vary by more than a factor of 20 over the total range of contour lengths. Our results support the hypothesis that shearing between protofilaments contributes significantly to the mechanics of microtubules.

PACS numbers: 87.15.Ya, 87.15.La, 87.16.Ka, 36.20.Ey

---

\* Corresponding author. FP and GL have equally contributed to this work.

The mechanics of living cells is determined by the cytoskeleton, a self-organizing and highly dynamic network of filamentous proteins of different lengths and stiffnesses [1]. Understanding the elastic response of purified cytoskeletal filaments is fundamental for the elucidation of the rheological behaviour of the cytoskeleton. Microtubules (MTs) are hollow cylindrical cytoskeletal filaments formed by in average thirteen tubulin protofilaments assembled in parallel. The outer and inner diameters are about 25 and 15 nm, respectively. In cells, MTs are generally 1 – 10  $\mu\text{m}$  long while in axons their length can be 50 – 100  $\mu\text{m}$  [2]. The tubular structure of MTs implies a minimal cross-sectional area, hence a high strength and stiffness combined with low density. Although usually modelled as isotropic cylinders, MTs have anisotropic elastic properties determined by their discrete protofilament structure. Their response to longitudinal tensile/compressive stress is determined by the strength of the head-tail  $\alpha\beta$ - $\alpha\beta$  tubulin bonds along the protofilament, whereas the response to shear stress by the weaker interprotofilament bonds [3, 4, 5, 6] which allow adjacent protofilaments to skew past each other (Fig 1b). In the language of continuum mechanics and linear elasticity theory, it is thus expected that the shear modulus  $G$  of MTs differs significantly from the Young’s modulus  $E$  [7, 8]. For instance, mechanically probing MTs with AFM yields a shear modulus that is 2-3 orders of magnitude smaller than the Young’s modulus [7, 8]. Moreover, a transversal buckling stress of  $P_r = 600$  Pa has been recently measured on MTs [9]. This is four orders of magnitude smaller than the buckling stress calculated by modelling MTs as isotropic solids with  $E \sim 1.6$  GPa. The main parameter for the description of the mechanics of polymer filaments is the ratio  $\ell_p/L$  between the persistence length  $\ell_p$  and the contour length  $L$ , which quantitatively describes the stiffness of a filament.  $\ell_p$  is expected to depend on both  $G$  and  $E$ , but a  $G \ll E$  implies also a dependence of  $\ell_p$  on  $L$ , as suggested by the recent AFM experiments in [8]. The most sensitive and elegant way to determine  $\ell_p/L$  is measuring the probability distribution function of the end-to-end distance of the filament,  $P(R)$  [10].  $P(R)$  and  $\ell_p/L$  have been measured with great accuracy for actin [11]. However, a detailed study of the mechanics of MTs based on probability distributions is complicated by their high stiffness, requiring an assay with very high spatial resolution. In this Letter, we describe a method based on single-particle tracking (SPT) for measuring the probability distribution function  $P(x, y)$  of grafted MTs. From the measured probability distributions we obtain the MTs persistence length and investigate its dependence on  $L$  over a broad range of contour lengths (2.6 – 48 $\mu\text{m}$ ). In the assay, single fluorescent colloidal beads are

attached at the tip of grafted MTs and the thermal fluctuations of the MT-bead system are recorded. Indeed, thermal fluctuations are the most natural way to mechanically probe biological nanometer-sized specimens non-destructively and over extended times. The experimental situation is depicted in Fig 1a. Biotinylated, rhodamine-labelled MTs, polymerized according to a standard protocol [12] and stabilized with taxol are covalently attached to a microstructured gold substrate made of parallel bars (bar width  $10\ \mu\text{m}$ , distance between the bars  $50\ \mu\text{m}$ ) (Fig 1a). The gold surface is chemically modified to ensure well-defined and reproducible conditions for the attachment of MTs [27]. A flow cell is assembled as shown in Fig 1a, setting a distance of  $20 - 30\ \mu\text{m}$  between the gold substrate and the upper and lower boundaries of the cell, so that any influence of the chamber's walls is negligible. A MTs suspension is then flowed into the cell perpendicularly to the bars, inducing MTs to attach preferentially along this direction, with just a segment of MT grafted to the grid, while the free portion fluctuates unconstrained in the medium (Fig 1a). A diluted suspension of yellow-green fluorescent, avidin-coated colloidal beads (diameter 200 or 500 nm, Molecular Probes F-8774 and Bang Laboratoires CP01F, respectively) is then flowed into the chamber. The beads bind strongly to the biotinylated MTs. Finally, the chamber is sealed with silicon grease, to avoid evaporation of the medium over time. In living cells, MTs usually irradiate from a microtubule organizing center toward the cell cortex [1], hence the boundary conditions adopted in our assay are close to MT configurations in cells. Single grafted MTs with one bead attached proximally to the tip are selected for the measurement. Alternatively, optical tweezers are employed to attach the bead to the MT's tip. Since the beads and the MTs emit fluorescence at two different wavelengths, they can be observed independently by exchanging the filter set in the microscope. Fig. 2a shows an example of the distribution resulting from the projection of the three-dimensional fluctuations of the MT's tip on the  $xy$  plane. The distribution is obtained by measuring the position of the fluorescent bead attached at the MT's end in at least  $10^4$  frames (average frame rate 16 frames/s). The bead's position is automatically tracked frame-by-frame with a custom particle-tracking routine. The coordinates of the bead's centroid can be determined with an accuracy of 1 nm and better under optimal conditions [13]. Here, the accuracy was slightly reduced to  $\sim 10$  nm. A stack containing the fluorescent MTs is recorded separately for the determination of  $L$ . The recorded particle position is used to obtain the probability distribution function  $P(x, y)$  of the free end in the  $xy$  plane and the corresponding reduced

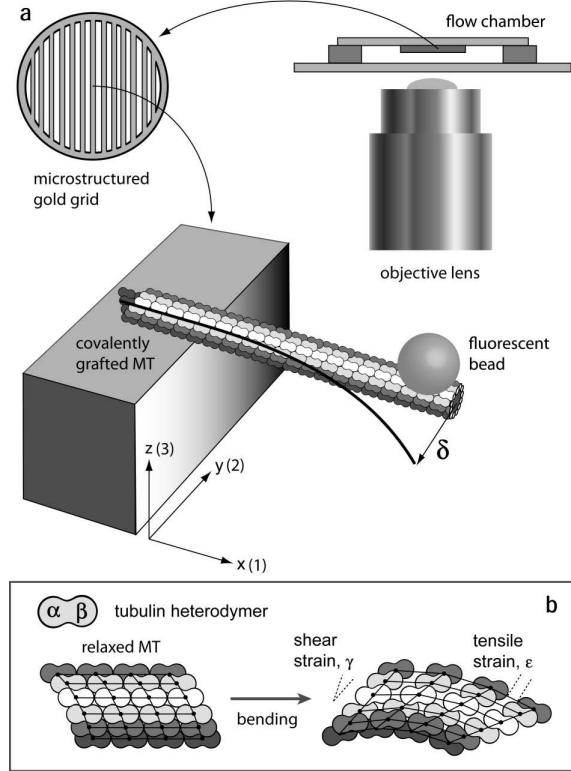


FIG. 1: Representation of the experimental situation. (a) The MT is covalently grafted on a gold substrate. A fluorescent colloidal bead (not to scale) is attached at the MT's tip, which freely fluctuates in the medium ( $\delta \equiv$  deflection). Both  $\delta$  and the MT bending profile are exaggerated for illustration purposes. The distance of the MT from both sides of the chamber is at least  $20 \mu\text{m}$ . (b) Bending generates a tensile/compressive stress  $P = E_1\epsilon$  and a shear stress  $s = G_{12}\gamma$  between adjacent protofilaments ( $E_1, G_{12}$  longitudinal Young's and shear modulus, respectively;  $\epsilon$  tensile strain,  $\gamma$  shear strain). Given the anisotropy in the tubulin interaction across and along protofilaments,  $E_1$  and  $G_{12}$  may differ by several orders of magnitude ( $x, y, z$  geometrical axes; 1, 2, 3 material axes).

distribution functions  $P(x)$  and  $P(y)$  (Fig. 2b-c), obtained by integrating  $P(x, y)$  over the coordinates  $y$  and  $x$  respectively [28]. These can be directly compared with theoretical predictions based on the wormlike chain model, as reported in [14]. Given the high persistence length of a microtubule ( $\ell_p/L$  can be as high as several hundreds), the longitudinal distribution function  $P(x)$  is peaked towards full stretching, as in Fig. 2c, and varies over a typical length scale  $L_{\parallel} = L^2/\ell_p$ . A non-Gaussian and asymmetric shape of  $P(x)$ , is clearly visible in Fig. 2b. In contrast,  $P(y)$  is a Gaussian whose width is given by the transverse length scale

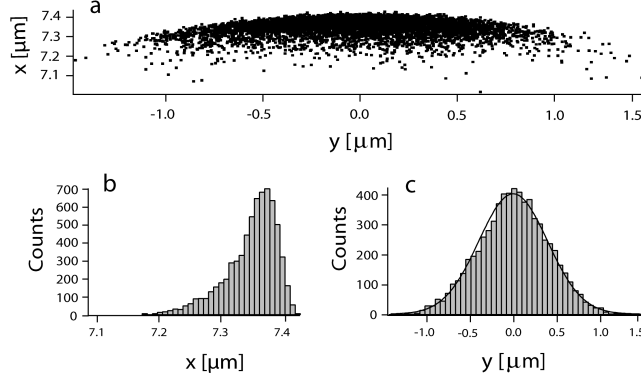


FIG. 2: (a) Bead's position tracked over  $10^4$  frames. The bead has a diameter of 200 nm and is attached at the tip of a MT with a contour length of  $7.2 \mu\text{m}$ . (b) Reduced distribution function along the x-axis (see Fig. 1a). (c) Reduced distribution function along the y-axis.

$L_{\perp} = \sqrt{(2L^3/3\ell_p)}$ , as represented in Fig. 2c [15, 16]. By measuring the contour length  $L$ ,  $\ell_p$  can be extracted from both  $P(x)$  or  $P(y)$ . It is important to notice that the measured  $P(x)$  and  $P(y)$  correspond to convolution products between the theoretical functions  $P_{th}(x)$  and  $P_{th}(y)$  predicted by the wormlike chain model [15, 16] and the function that represents the experimental precision in the measurement of the distance between the tip of the filament and the attachment point on the substrate. Since longitudinal and transverse fluctuations scale differently, the convolution has a negligible effect on  $P_{th}(y)$ , in contrast to  $P_{th}(x)$  whose shape is much more sensitive to small variations of the experimental precision. For this reason, we focused on  $P(y)$  for the determination of  $\ell_p$  in this work. The persistence lengths obtained from  $P(y)$  for 48 grafted microtubules of different contour lengths are shown in Fig. 3. We observe a clear dependence of  $\ell_p$  on  $L$ . This result is a direct consequence of the anisotropic tubulin interactions along and across protofilaments. In fact, as a consequence of their anisotropic protofilament structure, MTs are expected to have five independent elastic moduli across the longitudinal ( $xy$ ) and transversal ( $yz$ ) planes (i.e.  $E_1, E_2 = E_3$ ,  $G_{12} = G_{13}, G_{23}$ , and the Poisson's ratios  $\nu_{13} = \nu_{12}$ ; 1, 2, 3 are the material axes, Fig. 1a), similarly to fiber-reinforced materials [19]. In the following discussion we will model MTs as anisotropic hollow cylindrical beams and assume that the small fluctuations in the tip's position can be interpreted as deflections due to thermal forces. Given the boundary conditions and the geometry of the system, only the elastic moduli  $E_1$  and  $G_{12}$  are involved in bending on the  $xy$ -plane. Microscopically,  $E_1$  is expected to arise from the strong  $\alpha\beta$ - $\alpha\beta$  tubulin

bonds along single protofilaments, whereas the origin of  $G_{12}$  is expected to be in the much weaker interaction between tubulin dimers on adjacent protofilaments (see Fig. 1b), which are allowed to skew past each other in order to accommodate the shear strain associated with MTs bending. Thus, the total deflection of MTs ( $\delta$ ) is the sum of both bending ( $\delta_B$ ) and shear deformations ( $\delta_S$ ) [8, 17]:

$$\delta = \delta_B + \delta_S = \frac{PL^3}{\alpha E_1 I_2} + \frac{PL}{G_{12} k A} = \frac{PL^3}{\alpha \ell_p k_B T}, \quad (1)$$

where  $P$  is the lateral load at the MT's tip,  $I_2 = (1/4)\pi(R_e^4 - R_i^4)$  is the second moment of the tube's cross-sectional area  $A$ ,  $k$  a geometrical correction factor whose value is 0.72 for a hollow cylindrical beam [20], and  $\alpha = 3$  for a grafted beam. The last equality, with  $k_B T$  the thermal energy, represents the linear response of a semiflexible polymer [21]. Through the relation  $E_1 I_2 = \ell_p k_B T$ , Eq. 1 can be used to obtain the length dependence of the persistence length:

$$\ell_p = \ell_p^\infty \left( 1 + \frac{3E_1 I_2}{G_{12} k A L^2} \right)^{-1}, \quad (2)$$

where  $\ell_p^\infty$  is the persistence length for long microtubules ( $L \gg \sqrt{3E_1 I_2 / G_{12} k A} \simeq 21 \mu\text{m}$ ).

Eq. 2 provides a good fit to the experimental points, giving a value of  $\ell_p^\infty = 6.3 \pm 0.8$  mm in agreement with previous measurements on long MTs [22]. This value corresponds to  $E_1 = 1.51 \pm 0.19$  GPa and a ratio  $\delta_S / \delta_B = (21/L)^2$  when  $L$  is expressed in micrometers, corresponding to a ratio between Young's and shear modulus of  $\sim 10^6$ , three orders of magnitude higher than previously reported [7, 8]. This can be partially explained by the fact that in ref. [7, 8] MTs were stabilized with glutaraldehyde, a cross-linker used for chemical fixation of proteins, whereas we use the drug taxol, which insert in the MTs lattice and may relieve the internal tension inducing a further decrease of the shear modulus [23]. In addition, experiments reported in ref. [7, 8] suggest a strong dependence of the shear modulus on temperature. Whereas  $E \sim G$  in conventional materials, a shear modulus significantly smaller than the Young's modulus is typical of biological materials (from wood to bones) and engineered composites. Down to nanometer scale, a ratio  $E \setminus G \sim 10^2$  has also been measured for single-walled carbon nanotubes [24]. As shown in Fig. 3, the values of  $\ell_p$  measured on MTs spread with increasing  $L$ . This spreading is partially due to differences in the structures of single MTs. In facts, in MTs polymerized *in vitro* the

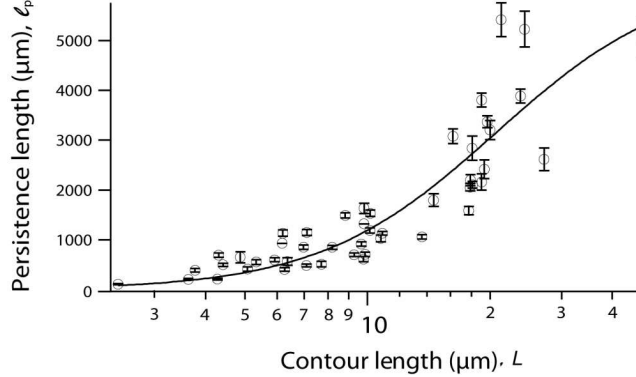


FIG. 3: The persistence length of MTs as a function of their contour lengths. The contour length ranges from  $2.6 \mu\text{m}$  to  $48 \mu\text{m}$ . The fit with Eq. 2 is superimposed on the experimental points.

number of protofilaments may vary from one MT to another and even along a given MT, and several lattice types are possible [25]. The probability of defects or inhomogeneities in the MT lattice may also increase with the contour length. Since there are also evidences that the stiffness of MTs can vary with the polymerization velocity [26], we carefully monitored the MT polymerization temperature. A further potential experimental source of error might be a loose binding of the bead to the MT, which could lead to an underestimation of  $\ell_p$ . This has been tested by pulling the bead with optical tweezers at high laser power, ensuring that it attaches firmly to the MT and does not roll or twist on it. In addition, by strongly bending the MT with optical tweezers we ensured that the segment of the MT anchored to the substrate does not change its orientation during thermal fluctuations, a further source of uncertainty in the measurement of  $L$ . Theoretical calculations show also that the fluctuations of the angle of torsion along the whole microtubule are below 7 degrees and can be safely neglected. In summary, we developed an assay based on single-particle tracking to measure with high spatial resolution the reduced distribution functions  $P(x)$  and  $P(y)$  for the tip's position of grafted MTs. Through a systematic measure of the persistence length of MTs with contour lengths between  $2.6$  and  $48 \mu\text{m}$ , we observe a dependence of the MTs stiffness on  $L$ . For short MTs ( $L = 2-3 \mu\text{m}$ )  $\ell_p$  is at least one order of magnitude smaller than for long ones ( $L \geq 30-40 \mu\text{m}$ ). This property can be explained by the anisotropic structure of MTs, and described by linear elasticity theory. Our results together with those in [7, 8, 9] suggest that the interprotofilament bonds are much weaker than the  $\alpha\beta$ - $\alpha\beta$  tubulin bonds along the protofilaments, leading to a very low shear modulus in MTs. The dependence of  $\ell_p$  on  $L$  in

MTs might also contribute to explain the broad range of measured MTs persistence lengths found in literature (0.5–5 mm) [22, 23, 26]. Noticeably, the maximum variability of  $\ell_p$  occurs at contour lengths close to the typical length scale of a cell ( $L \simeq 12 \mu\text{m}$ ). It is interesting to speculate about the biological significance of this property. MTs are able to accomplish various tasks in differently sized cells and during different stages of a cell's life cycle. On one hand, flexibility of MT's tip allows MTs to search space laterally for binding partners or to bend and continue growing in a modified direction when encountering obstacles, for example when growing MTs hit the side of a small fission yeast cell. On the other hand, sufficient rigidity is important in situations in which MTs need to resist to pushing forces such as in large vertebrate cells during anaphase of mitosis, when the spindle elongates. The length dependence of MTs rigidity might have allowed cells during evolution to use MTs in an optimal way both for lateral searching and for exerting pushing forces in different contexts and especially on different length scales. We are grateful to A. Rohrbach, E. H. K. Stelzer and J. Swoger for their substantial support and many interesting discussions. GL's research has been partially supported by a Marie Curie Fellowship under contract no. HPMF-CT-2001-01432. FP has been supported by the German Research Foundation, grant no. FL351/2-1.

- 
- [1] F. Nédélec et al., *Curr. Op. Cell Biol.* **15**, 118 (2003).
  - [2] D. Bray, *Cell Movements - from molecules to motility* (Garland Publishing, New York, 2001).
  - [3] D. Van Buren et al., *Proc. Natl. Acad. Sci. USA* **99**, 6035 (2002).
  - [4] P. J. de Pablo et al., *Phys. Rev. Lett.* **91**, 098101 (2003).
  - [5] I. A. T. Schaap et al., *Eur. Biophys. J.* **33**, 462 (2004).
  - [6] D. Sept et al., *Protein Sci.* **12**, 2257 (2003).
  - [7] S. Kasas et al., *ChemPhysChem* **5**, 252 (2004).
  - [8] A. Kis et al., *Phys. Rev. Lett.* **89**, 1216 (2002).
  - [9] D. J. Needleman et al., *Phys. Rev. Lett.* **93**, 198104 (2004).
  - [10] J. Wilhelm and E. Frey, *Phys. Rev. Lett.* **77**, 1216 (1996).
  - [11] L. LeGoff et al., *Physical Review Letters* **89**, 258101 (2002).
  - [12] K. L. Carraway and C. A. C. Carraway, *The Cytoskeleton – a practical approach* (Oxford



- University Press, New York, 1992).
- [13] M. Speidel et al., *Opt. Lett.* **28**, 69 (2003).
- [14] G. Lattanzi et al., *Phys. Rev. E* **69**, 021801 (2004).
- [15] P. Benetatos and E. Frey, *Phys. Rev. E* **67**, 051108 (2003).
- [16] J. Wilhelm and E. Frey, unpublished.
- [17] S. Timoshenko and J. N. Goodier, *Theory of Elasticity* (McGraw-Hill, New York, 1970).
- [18] L. D. Landau and E. M. Lifshits, *Course of Theoretical Physics, Vol. 7* (Pergamon Press, London, 1959).
- [19] L. P. Kollár and G. S. Springer, *Mechanics of Composite Structures* (Cambridge University Press, 2003).
- [20] A. Kis, *Doctoral Thesis* (EPFL, Lausanne <http://library.epfl.ch/theses>, 2003) p. 118.
- [21] K. Kroy and E. Frey, *Phys. Rev. Lett.* **77**, 306 (1996).
- [22] F. Gittes et al., *J. Cell. Biol.* **120**, 923 (1993).
- [23] H. Felgner et al., *J. Cell. Sci.* **109**, 509 (1996).
- [24] J. P. Salvetat et al., *Phys. Rev. Lett.* **82**, 944 (1999).
- [25] D. Chrétien et al., *J. Cell. Biol.* **117**, 1031 (1992).
- [26] M. E. Janson, and M. Dogterom, *Bioph. J.* **87**, 2723 (2004).
- [27] The grid surface is cleaned with a solution  $\text{H}_2\text{O}_2/\text{NH}_3/\text{H}_2\text{O}$  1:1:5 and incubated overnight with mercaptoundecanoic acid (5 mM in ethanol), producing a self-assembled monolayer with exposed carboxylic groups. These are activated by an aqueous solution of N-hydroxysuccinimide and 1-ethyl-3-(3-dimethylaminopropyl)carbodiimide both 100 mM to ensure the covalent attachment of MTs.
- [28] According to [11] the longest relaxation time for a semiflexible polymer is  $\tau_C = (\zeta/\ell_p k_B T)(L/A)^4$ , where  $\zeta = 2.47 \times 10^{-3}$  Pa s is an effective friction coefficient and  $A = 1.875$  for a polymer with one clamped and one free end. We find that  $\tau_c = 76.6$  ms for a MT of 10  $\mu\text{m}$ : end-to-end fluctuations saturate quite fast to the equilibrium value within the time of the observation